Cell, Vol. 105, 781–792, June 15, 2001, Copyright ©2001 by Cell Press

Smoothened Mutants Reveal Redundant Roles for Shh and Ihh Signaling Including Regulation of L/R Asymmetry by the Mouse Node

Xiaoyan M. Zhang,[2] Miguel Ramalho-Santos, and Andrew P. McMahon[1]
Department of Molecular and Cellular Biology
The Biolabs
Harvard University
16 Divinity Avenue
Cambridge, Massachusetts 02138

Summary

Genetic analyses in *Drosophila* have demonstrated that the multipass membrane protein Smoothened (Smo) is essential for all Hedgehog signaling. We show that *Smo* acts epistatic to *Ptc1* to mediate Shh and Ihh signaling in the early mouse embryo. *Smo* and *Shh/Ihh* compound mutants have identical phenotypes: embryos fail to turn, arresting at somite stages with a small, linear heart tube, an open gut and cyclopia. The absence of visible left/right (L/R) asymmetry led us to examine the pathways controlling L/R situs. We present evidence consistent with a model in which Hedgehog signaling within the node is required for activation of *Gdf1*, and induction of left-side determinants. Further, we demonstrate an absolute requirement for Hedgehog signaling in sclerotomal development and a role in cardiac morphogenesis.

[Dedicated to Rosa Beddington, a pioneer in mammalian embryology].

Introduction

Hedgehog (HH) signaling plays many distinct roles in the development of *Drosophila* and vertebrate embryos (reviewed in Hammerschmidt et al., 1997). In the fly, there is a single *HH* gene. In contrast, three different genes, *Sonic* (*Shh*), *Indian* (*Ihh*), and *Desert* (*Dhh*) *hedgehog* play distinct regulatory roles in mammals. Shh has been shown to regulate pattern in the somite (Fan and Tessier-Lavigne, 1994; Fan et al., 1995; Chiang et al., 1996; Kos et al., 1998), neural tube (Echelard et al., 1993; Chiang et al., 1996; Liu et al., 1998; Ye et al., 1998; Dutton et al., 1999; Rowitch et al., 1999; Wechsler-Reya and Scott, 1999; Wallace, 1999), and limb (Parr and McMahon, 1995; Masuya et al., 1995; Chiang et al., 1996; Zuniga et al., 1999), as well as growth and morphogensis of several organs including hair (St-Jacques et al., 1998; Chiang et al., 1999; Sato et al., 1999), tooth (Dassule and McMahon, 1998; Dassule et al., 2000; Sarkar et al., 2000; Zhang et al., 2000), lung (Litingtung et al., 1998; Pepicelli et al., 1998), and gut (Apelqvist et al., 1997; Ramalho-Santos et al., 2000; Hebrok et al., 2000). *Ihh* plays a central role in coordinating growth and differentiation of chondrocytes in the developing endochondral skeleton (Vortkamp et al., 1996; St-Jacques et al., 1999; Karp et al., 2000) and also regulates the mammalian gut (Ramalho-Santos et al., 2000). Finally, *Dhh* is required for spermatogenesis (Bitgood et al., 1996) and development of the perineurial sheath that encases peripheral nerves (Parmantier et al., 1999).

Biochemical studies indicate that Patched (Ptc), a multipass membrane protein with homology to sterol-sensing proteins, is a HH receptor (Marigo et al., 1996; Stone et al., 1996). How HH binding to Ptc activates HH signaling is not entirely clear. Genetic studies indicate that Ptc is required to inhibit the activity of a second multipass membrane protein, Smoothened (Smo) (Chen and Struhl, 1996; Quirk et al., 1997). In the absence of Ptc, ligand-independent activation of HH targets depends, as does all normal HH signaling, on the activity of Smo. Thus, Ptc inhibits the activity of Smo and HH binding to Ptc releases Smo from this inhibitory process.

Recent studies in the fly have shed light on these interactions. Ptc regulates the stability, membrane accumulation, and phosphorylation state of Smo (Alcedo et al., 2000; Denef et al., 2000; Ingham et al., 2000; Strutt et al., 2001). When HH binds to Ptc, Smo accumulates in the membrane in a highly phosphorylated state and HH targets are activated. In the absence of ligand, Smo is less phosphorylated and rapidly turns over. Although initial studies argued that Ptc and Smo might act together in a receptor complex (Stone et al., 1996), it now appears likely that Ptc regulates Smo indirectly through a nonstochiometric mechanism (Denef et al., 2000). Finally, new evidence suggests a Ptc-independent pathway of HH signaling which would indicate that there is another HH receptor (Denef et al., 2000; Ramirez-Weber et al., 2000).

At least two *Ptc* genes exist in mammals. Loss of function in the first of these to be identified, *Ptc1*, leads to constitutive activation of HH targets, suggesting a conservation in HH signaling mechanisms from flies to vertebrates (Goodrich et al., 1997). Ptc2 also binds all mammalian HHs, but whether it actually plays a role in HH signal transduction is not clear (Carpenter et al., 1998). *Smo* is represented by a single mammalian homolog (Stone et al., 1996; Akiyama et al., 1997). The identification of activated forms of Smo in some basal cell carcinomas, where HH targets are constitutively expressed, suggests that Smo also plays a role in regulating HH signaling in mammals (Xie et al., 1998). Further, ectopic expression of this oncogenic form of Smo appears to lead to cell-autonomous activation of HH targets in the neural tube, consistent with Smo playing a positive role in the transduction of a HH signal (Hynes et al., 2000). Here, we explore the role of Smo in HH signaling in the early somite stage mouse embryo.

Results

Genetic Analysis of *Smo* Function in Mice

To gain an insight into the role of Smo in HH signaling in vertebrates, we generated a null allele of *Smo* by gene

[1] Correspondence: amcmahon@mcb.harvard.edu
[2] Present address: Curis Inc., 45 Moulton Street, Cambridge, Massachusetts 02138.

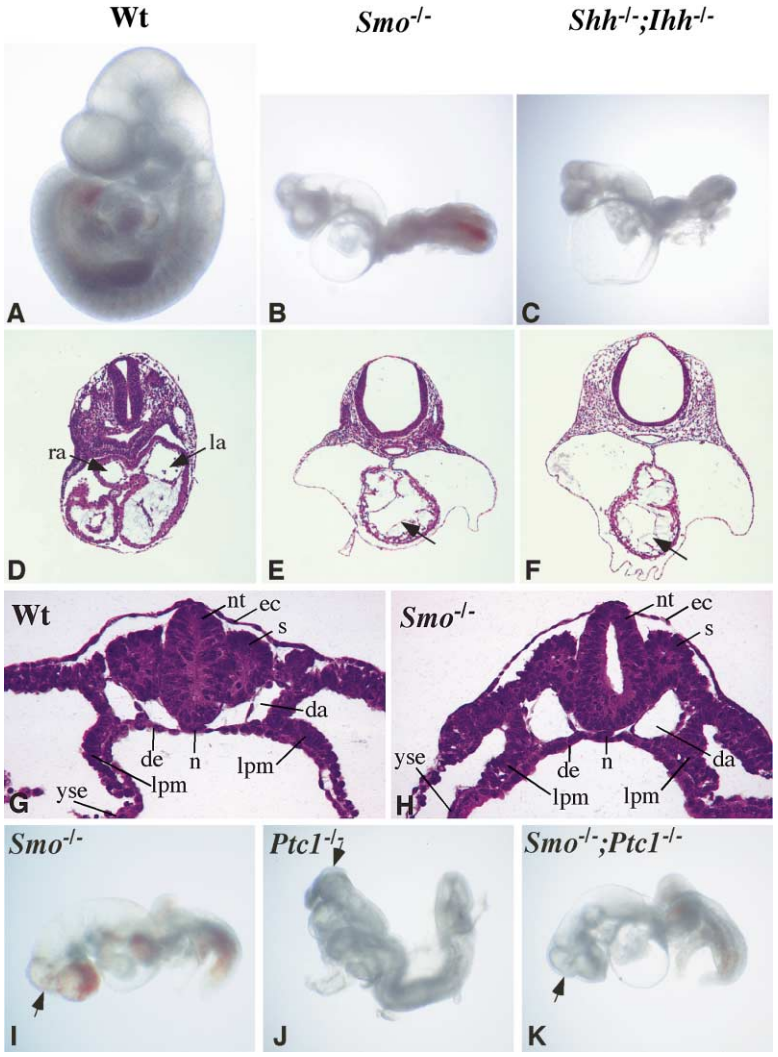

Figure 1. A *Smo* Null Mutant Phenocopies *Shh*/*Ihh* Compound Mutants and *Smo* Is Epistatic to *Ptc1*

External morphology of 9.5 dpc embryos: (A) wild-type; (B) $Smo^{-/-}$; (C) $Shh^{-/-}$;$Ihh^{-/-}$. Cross-sections of 9.5 dpc (D) wild-type; (E) $Smo^{-/-}$; (F) $Shh^{-/-}$;$Ihh^{-/-}$ embryos at the level of the heart tube. Left (la) and right (ra) atria are indicated in the wild-type, and the linear heart tube of *Smo* and *Shh*/*Ihh* compound mutants are arrowed. Cross-sections through the trunk region of 9 somite stage wild-type (G) and *Smo* mutant (H) embryos indicate that all major cell types are present in a grossly normal organization in the *Smo* mutant (da, dorsal aorta; de, definitive endoderm; ec, ectoderm; lpm, lateral plate mesoderm; n, notochord; nt, neural tube; s, somite; yse, yolk sac endoderm). External morphology of 9.5 dpc embryos: (I) $Smo^{-/-}$; (J) $Ptc1^{-/-}$; (K), $Smo^{-/-}$;$Ptc1^{-/-}$. Note the closed brain vesicles of the *Smo* mutant and *Smo*/*Ptc1* compound mutant and the open ventralized brain of the *Ptc1* mutant (arrows).

targeting in mouse embryonic stem (ES) cells (Supplementary Figure S1 at http://www.cell.com/cgi/content/full/105/6/781/DC1). Mice heterozygous for the *Smo* mutation had no discernible phenotype. However, in contrast to homozygous null mutants in *Shh*, *Ihh*, or *Dhh* which develop to term, *Smo* mutants did not survive beyond 9.5 days post coitum (dpc). *Smo* mutants exhibited ventral cyclopia and holoprosencephaly, which are also observed in *Shh* mutants, consistent with Smo playing an essential role in transduction of a Shh signal (Chiang et al., 1996). In addition, *Smo* mutants failed to undergo embryonic turning, closure of the ventral midgut, and normal rightward looping of the heart, which remained as a linear tube (compare Figures 1A, 1D and 1B, 1E). *Smo* mutants were first distinguishable at the 6–7 somite stages by the abnormal shape of the forebrain, indicative of the loss of ventral midline fates and by a delay in cardiac morphogenesis. *Smo* mutants showed no general growth or developmental retardation at this time, relative to their wild-type littermates. Analysis of sections through the trunk region of 9 somite stage embryos (Figures 1G and 1H) indicated that the general organization of all major cell populations (neural, ectodermal, mesodermal, and endodermal) appeared grossly similar to wild-type embryos. By the 13 somite stage, *Smo* mutants showed signs of growth retardation. This phenotype was independent of whether a chorio-allantoic connection was established and may result in part from defective cardiac function. In summary, the loss-of-function phenotype indicates that the role of Smo in the early mouse embryo is not confined to transduction of a Shh signal.

To determine whether Smo's role in Hedgehog signaling may have diverged between flies and mice, we examined the relationship between *Smo* and *Ptc1*. Ectopic activation of *Shh* targets in *Ptc1* mutants results in a ventralized neural plate, which fails to close in the head region, and an abnormal expansion of somites (Figure 1J; Goodrich et al., 1997). In contrast, compound mutants in *Smo* and *Ptc1* at the same stage (Figure 1K) displayed a phenotype indistinguishable from *Smo* mutants (Figure 1I). Thus, *Smo* is epistatic to *Ptc1*, demonstrating conservation of the genetic hierarchies regulating HH signaling in flies and mice (Chen and Struhl, 1996; Quirk et al., 1997).

The differences observed between *Smo* and *Shh* mu-

tants could indicate that Smo plays additional roles in the transduction of other HH signals in the early somite stage mouse embryo. As *Ihh* and *Dhh* mutants have no observable phenotype at early somite stages (Bitgood et al., 1996; St-Jacques et al., 1999), any additional HH signaling would most likely reflect redundant signaling by more than one HH family member. *Ihh* is widely expressed in the yolk sac endoderm and developing embryonic gut endoderm at somite stages (Bitgood and McMahon, 1995). To determine whether Shh and Ihh have redundant signaling roles, we analyzed compound mutants in *Shh* and *Ihh*. Compound mutants exhibited a more severe phenotype than *Shh* mutants, one that is indistinguishable from the *Smo* mutant phenotype (compare Figures 1B, 1E and 1C, 1F). These results indicate that Smo is essential for the transduction of both Shh and Ihh signals. Further, these two family members play hitherto unappreciated roles in the somite stage mouse embryo.

Expression of *Shh*, *Ihh*, and *Ptc1* in Early Mouse Development

As a first step toward addressing the additional roles of *Shh* and *Ihh*, we performed a detailed analysis of their expression with respect to HH signaling in mouse embryos collected from pre-somite to early somite stages (7.5–8.5 dpc). Expression of *Shh* in the node, midline mesoderm of the head process, and notochord (Figures 2A and 2F) and gut endoderm (Figure 2K) has previously been reported (Echelard et al., 1993; Bitgood and McMahon, 1995; Ramalho-Santos et al., 2000). *Ihh* is strongly expressed in the visceral endoderm of the yolk sac (Figures 2B and 2G; Bitgood and McMahon, 1995). In addition, we found a new site of weak *Ihh* expression in the posterior part of the node at 7.75–8.0 dpc (Figures 2B and 2G), demonstrating that *Shh* and *Ihh* are coexpressed in the node. Whether they are coexpressed in the same cell population or in immediately adjacent cell types is not clear. Upregulation of *Ptc1,* a general transcriptional target of HH signaling, in the yolk sac mesoderm, the periphery of the node, and at the midline suggests that Shh and Ihh signaling is occurring at this stage (Figures 2C and 2H). Importantly, we did not detect any L/R asymmetry in the expression of *Shh*, *Ihh*, or *Ptc1*. *Smo* is expressed strongly throughout the embryo (data not shown).

To address whether Shh and Ihh play redundant roles in HH signaling in the mouse node, we analyzed *Ptc1* expression in *Shh* mutants. As expected, no induction of *Ptc1* was observed at the midline of *Shh* mutant embryos, but expression was maintained in the posterior node (Figures 2D and 2I). In contrast, when all HH signaling was removed in *Smo* mutants, the upregulation of *Ptc1* in the node was abolished (Figures 2E and 2J). Thus, both Shh and Ihh signal within the node in a Smo-dependent mechanism.

By early somite stages (8.5 dpc), coexpression of *Shh* and *Ihh* was also observed in two lateral domains of definitive endoderm (Figures 2K and 2L). *Ptc1* responsiveness was monitored by expression of a $Ptc1^{lacZ}$ allele (Goodrich et al., 1997). In embryos heterozygous for this allele, *Ptc1* was upregulated in the lateral mesoderm, ventral neural tube, and somites, reflecting the activation of HH pathways in these tissues (Figure 2M). Shh signaling at the midline is known to regulate dorsal/ventral pattern within the neural tube and somites (reviewed in Hammerschmidt et al., 1997). However, although no upregulation of *Ptc1* was detected in the ventral neural tube of *Shh* mutants at 8.5 dpc as expected (Figure 2N), *Ptc1* was upregulated within the somites and lateral plate mesoderm (Figure 2N) in a Smo-dependent mechanism (Figure 2O). Together, these findings suggest that Shh and Ihh have redundant signaling activities in the node, somites, and lateral plate mesoderm.

Shh and Ihh Regulate L/R Asymmetry

The absence of turning and heart looping in *Smo* and *Shh/Ihh* compound mutants, together with the coexpression of *Shh* and *Ihh* in the node, a structure central to the establishment of L/R asymmetry, prompted us to investigate the pathways of L/R determination. *Pitx2*, which encodes a bicoid-related homeobox gene, is expressed asymmetrically in the left lateral plate mesoderm by 6–8 somite stages (Figure 3A; Piedra et al., 1998; Ryan et al., 1998; Yoshioka et al., 1998). This asymmetry is conserved across vertebrates and is required for the asymmetric development of organ situs (for review see Burdine and Schier, 2000; Capdevila et al., 2000). In contrast, in the head and yolk sac, *Pitx2* is expressed bilaterally (Figure 3A). As previously described (Meyers and Martin, 1999), *Pitx2* is expressed bilaterally in the lateral plate mesoderm of *Shh* mutants (Figure 3B), most likely due to a failure of Shh-mediated induction of the floor plate. The floor plate is thought to regulate maintenance, but not initiation, of L/R asymmetry (see Discussion). *Ihh* mutants display a wild-type pattern of *Pitx2* expression confined to the left lateral plate mesoderm (Figure 3C). Surprisingly, no expression *of Pitx2* was detected in the lateral plate mesoderm of either *Shh/Ihh* compound mutants or *Smo* mutants, whereas expression in the head mesenchyme and yolk sac was unaltered (Figures 3D and 3E).

These results suggest that HH signaling is required for the induction of asymmetric gene expression in the left lateral plate mesoderm and that either Shh or Ihh is sufficient for this process. To determine whether HH signaling acts directly in the lateral plate mesoderm, we used *Ptc1* mutants to upregulate HH signaling. Loss of *Ptc1* activity results in constitutive activation of HH targets (including *Ptc1* itself) in all HH responsive cells (Goodrich et al., 1997). Therefore, if HH signaling is sufficient for activation of *Pitx2* in the lateral plate mesoderm, one would expect ectopic activation of *Pitx2* in the right lateral plate mesoderm of *Ptc1* mutants. In contrast, *Pitx2* expression remained confined to the left lateral plate mesoderm in *Ptc1* mutant embryos (Figure 3F) even though the strong bilateral upregulation of *Ptc1* indicated ectopic HH signaling in the lateral plate mesoderm (data not shown).

To investigate in greater depth the role of HH signaling in mouse L/R axis development, we focused our analyses on *Smo* mutants at 2–8 somite stages, the period when asymmetric expression of L/R gene expression is first observed. *TGF*β family members *Nodal*, *Lefty1*, and *Lefty2* are three conserved, essential components of the

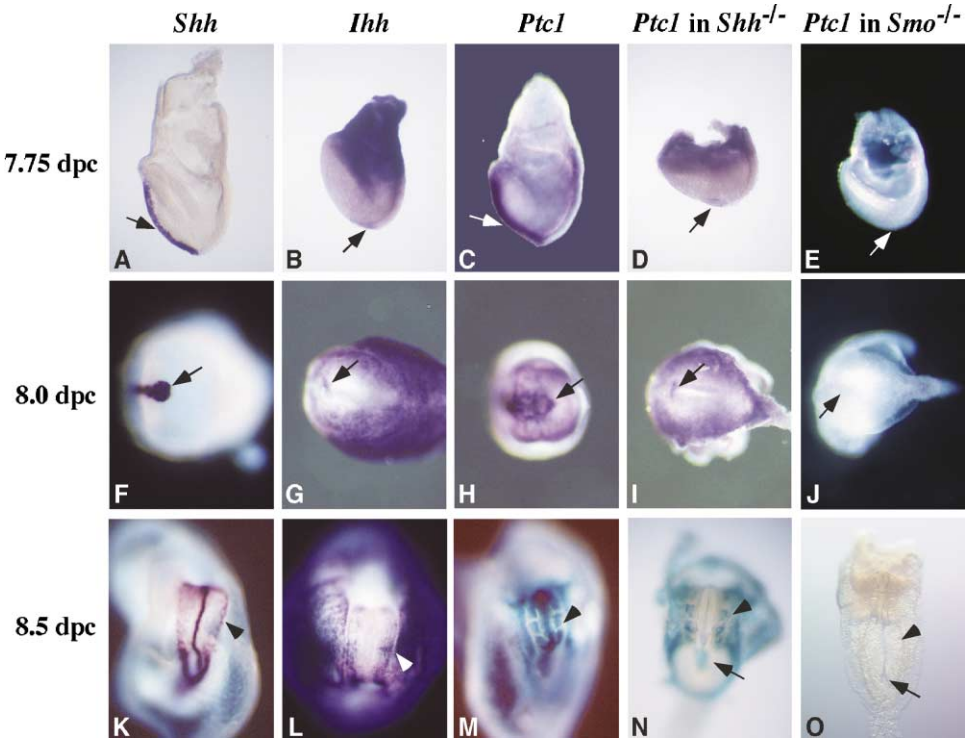

Figure 2. Analysis of *HH* Gene Expression and *HH* Response in the Early Mouse Embryo

Expression of *Shh*, *Ihh*, and *Ptc1* during early mouse development. Whole-mount in situ hybridization to 7.75 dpc pre-somite stage embryos (A–E, lateral view; anterior is to the left). The anterior neural plate (left) which overlies the midline mesoderm and the posterior primitive streak region (right) are visible. Whole-mount in situ hybridization to 8.0 dpc embryos (F–J, ventral view; anterior is to the left). In this view, the node (arrow) is clearly visible, the notochord extends anterior (left), and the primitive streak posterior (right) to the node. Whole-mount in situ hybridization (K and L) and whole-mount β-galactosidase histochemistry (M–O) as performed on 8.5 dpc embryos are shown (K–O, ventral view; anterior is up). (A, F, and K) *Shh* expression; (B, G, and L) *Ihh* expression; (C–E) and (H–J) *Ptc1* expression. (M–O) β-galactosidase activity from a $Ptc1^{lacZ}$ allele. All the embryos used were wild-type except for $Shh^{-/-}$ in (D) and (I), $Smo^{-/-}$ in (E) and (J), $Ptc1^{lacZ/+}$ (M), $Shh^{-/-}$; $Ptc1^{lacZ/+}$ in (N), and $Smo^{-/-}$; $Ptc1^{lacZ/+}$ in (O). Arrows in (A) and (C) indicate expression in the midline. Arrows in (B), (D), (E)–(J), (N), and (O) indicate expression in the node. Arrowheads indicate expression in the endoderm (K and L) and expression in the somite (M–O).

L/R asymmetry pathway whose asymmetric expression is highly conserved across vertebrate groups (reviewed in Burdine and Schier, 2000; Capdevila et al., 2000). In wild-type embryos, *Nodal* is expressed in the left lateral plate mesoderm and in the periphery of the node (Figure 3G). Within a narrow time window (5–6 somite stages), *Nodal* is also expressed more strongly on the left side of the node; the significance of this asymmetry is unclear (Figure 3G; Collignon et al., 1996). In all *Smo* mutants, *Nodal* expression was absent from the lateral plate mesoderm (Figure 3H). Although expression was retained in the node, expression levels in the node were highly variable, some embryos even displayed higher levels of *Nodal* expression on the right side of the node. In *Ptc1* mutants, *Nodal* expression was unaltered in the lateral plate mesoderm or the node, suggesting that *Nodal* is indirectly regulated by HH signaling (Figure 3I). Finally, *Lefty2* is normally expressed in the left lateral plate mesoderm and *Lefty1* in the left floor plate at 3–6 somite stages (Figure 3J), but neither was expressed in *Smo* mutants at the same stages (Figure 3K). *Lefty2* expression in the left lateral plate mesoderm is a target of Nodal signaling (reviewed in Shen and Schier, 2000), whereas expression of *Lefty1* in the floor plate requires the prior induction of floor plate cells, a Shh-dependent patterning process (Chiang et al., 1996). These two observations explain the absence of *Lefty* expression in *Smo* mutants.

The failure to activate a left-side specific pathway of factors in *Smo* mutants did not result from a general failure of lateral plate mesoderm development. Bilateral expression of *Bmp4* (Figures 3L and 3M), *Twist* (Figures 3N and 3O), and *Hoxb6* (data not shown) at the 2–8 somite stages indicated that the lateral mesoderm was present and grossly normal in *Smo* mutants. In summary, the data indicate that a Shh/Ihh signaling pathway lies upstream of the activation of left-sided gene expression in the lateral plate mesoderm. However, HH signaling in the lateral plate may not directly regulate this pathway. Both Shh and Ihh signal within the node, suggesting that HH signaling in the node might play a role in the subsequent activation of a left-side specific pathway of regulatory factors in the lateral plate mesoderm.

HH Signaling Controls the Expression of *Gdf1* and Cryptic

Gdf1 encodes a TGFβ family member that acts upstream of *Nodal*, *Lefty1/2*, and *Pitx2* (Rankin et al., 2000). At 2–8 somite stages, *Gdf1* is expressed symmetrically in the node, the ventral neural tube, and intermediate and lat-

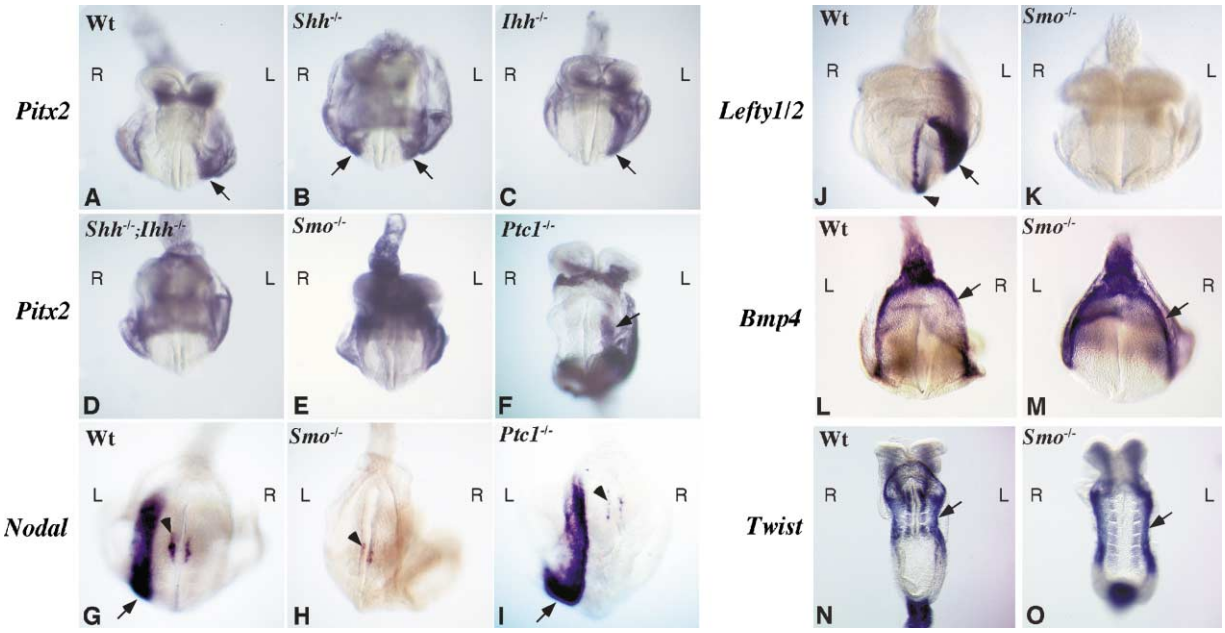

Figure 3. HH Signaling Regulates Expression of a Left-Sided Cascade of Regulatory Factors

Whole-mount in situ hybridization analysis of the expression of left-side markers in mouse embryos deficient in different members of the HH signaling pathway (as indicated). Ventral anterior view of embryos following in situ hybridization with a *Pitx2* probe (A–F) and *Lefty1/2* (J and K) probe is shown. (G)–(I) are ventral posterior views of embryos showing *Nodal* expression. (L) and (M) are ventral posterior views of *Bmp4* expression and (N) and (O) are ventral views (anterior up) of *Twist* expression in the lateral plate mesoderm. Gene expression in the lateral plate mesoderm is indicated by an arrow, and expression in the node by arrowheads, in all panels.

eral plate mesoderm (Rankin et al., 2000; Figure 4A). Although it is not clear which *Gdf1* expression domain is responsible for regulating the left-side specific pathway, early expression in the node is likely to be important. *Gdf1* expression was examined in *HH* pathway mutants at 2–8 somite stages. *Gdf1* is significantly downregulated in the node and ventral neural tube of *Shh* mutant embryos, but only slightly reduced in intermediate and lateral plate mesoderm (Figure 4B). Expression of *Gdf1* was maintained in the node and at the midline in *Ihh* mutants, but lateral mesoderm expression was downregulated (Figure 4C). Interestingly, *Gdf1* expression was completely absent in the node of *Smo* mutants and expression was downregulated in other expression domains (Figure 4D), indicating that *Gdf1* is a target of Shh and Ihh signaling. In support of this conclusion, *Gdf1* underwent a dramatic upregulation throughout its normal expression domain in *Ptc1* mutant embryos (compare Figure 4E with 4F).

Cryptic, a member of the EGF-CFC family of extracellular factors, is an essential cofactor in Nodal-mediated induction of *Lefty2* within the left lateral plate mesoderm (Gaio et al., 1999; Yan et al., 1999). Cryptic is normally expressed symmetrically in the lateral plate mesoderm, node, notochordal plate, and prospective floor plate (Yan et al., 1999; Figure 4G). Cryptic expression was absent in the prospective floor plate and greatly reduced in both the node and lateral plate mesoderm of *Smo* mutant embryos at 2–6 somite stages (Figure 4H). In contrast, Cryptic was upregulated in the ventral neural tube and node, and ectopically activated in the anterior primitive streak of *Ptc1* mutant embryos (Figure 4J). Thus, Cryptic, like *Gdf1*, appears to be a target of HH signaling.

Defective Heart Morphogenesis in *Smo* Mutants

Loss-of-function mutants in most genes that regulate L/R asymmetry randomize the process of heart looping. Thus, these genes are not essential for looping, but instead bias the direction of looping so that the heart normally loops to the right. In contrast, the heart of *Smo* mutants remained as a linear tube (Figure 1E). This phenotype might indicate that *Smo* mutants are unable to break bilateral symmetry. Alternatively, HH signaling could also play an independent role in cardiac morphogenesis. In support of this latter view, heart development was retarded in early somite stage *Smo* mutants (data not shown), a phenotype not reported in other mutants with defective L/R situs. Previous studies have demonstrated that the homeobox containing transcriptional regulator Nkx2.5 is essential for normal heart morphogenesis, and cardiac myogenesis (Lyons et al., 1995). In wild-type embryos, at early head-fold stages (2–3 somite stages), *Nkx2.5* is expressed at high levels in cardiac mesoderm (Figures 5A and 5C). Later, expression is observed throughout the myocardial layer of the heart tube (Figure 5G). In contrast, *Nkx2.5* expression was barely detectable in *Smo* mutant embryos at 2–3 somite stages (Figure 5B). Further, its expression domain was upregulated in *Ptc1* mutants (Figure 5D). Expression of *Wnt2* (Monkley et al., 1996), another cardiac marker, was unaltered (Figures 5E and 5F). Thus, *Nkx2.5* appears to be a specific cardiac target of HH signaling and the reduced levels of *Nkx2.5* activity might underlie

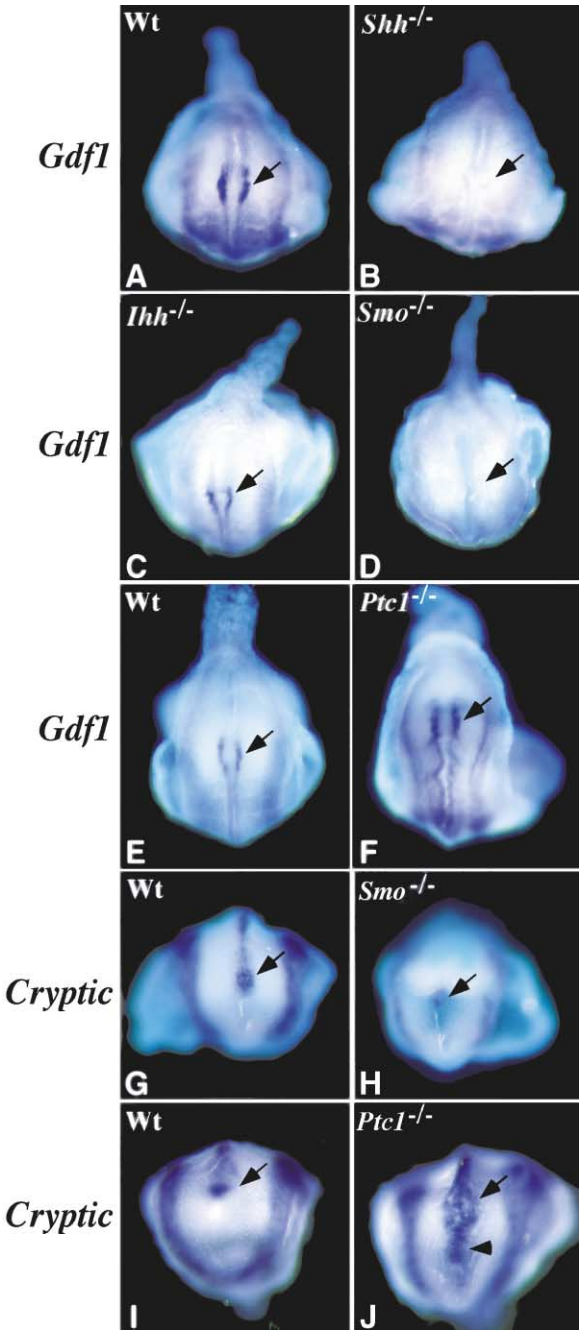

Figure 4. Expression of *Gdf1* and *Cryptic* in the Mouse Node Is under HH Control

Whole-mount in situ hybridization at 8.5 dpc shows that *Gdf1* expression in the node (arrow) is dramatically reduced in *Shh* mutants, slightly downregulated in *Ihh* mutants, undetectable in *Smo* mutants, and upregulated in *Ptc1* mutants (A–F, ventral posterior views of node and primitive streak [up] region). Histochemical staining of embryos in (E) and (F) was for identical times, but the incubation period was shorter than for the wild-type embryo in (A) to highlight the upregulation of *Gdf1*in *Ptc1* mutants. The wild-type embryos Cryptic expression (G) is downregulated in the lateral plate mesoderm and node (arrow) and absent in the ventral neural tube of *Smo* mutants (H). Cryptic expression (I) is expanded in the midline and node region (arrow) and ectopically activated in the anterior primitive streak of *Ptc1* mutants (arrowhead in [J]). (G)–(J) are ventral views focusing on the node region (primitive streak is down).

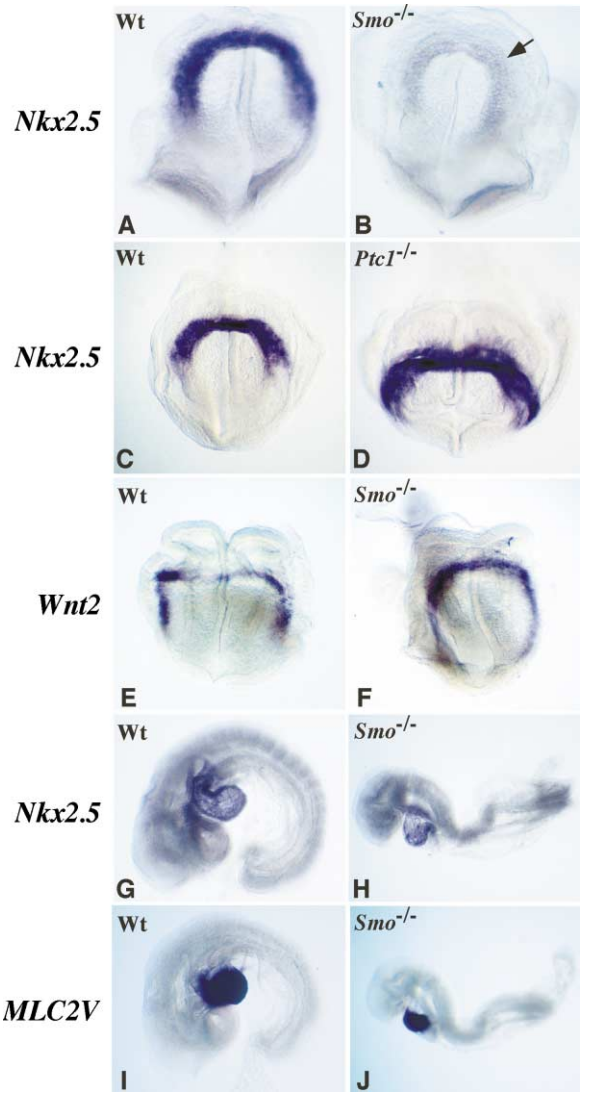

Figure 5. Reduced Expression of *Nkx2.5* in the Absence of HH Signaling Correlates with a Failure of Heart Looping

Expression of *Nkx2.5* in early cardiac progenitor cells (A) is significantly reduced in early head-fold stage *Smo* mutants (B), and the wild-type expression domain (C) is expanded in *Ptc1*mutants (D). A second cardiac mesoderm marker, *Wnt2,* is expressed at similar levels in wild-type (E) and *Smo* mutant (F) embryos. Normal levels of *Nkx2.5* are established by 9.0 dpc (compare [G] and [H]), and the ventricle-specific myosin light chain gene *MLC-2V*, a target of *Nkx2.5* regulation, is expressed in *Smo* mutants (compare [I] and [J]). (A)–(F) are ventral anterior views (head folds up) and (G)–(J) are lateral views of embryos following whole-mount in situ hybridization with the indicated probes.

the defective heart morphogenesis observed in *Smo* mutants. At later stages (approximately 16–18 somites; Figure 5H), *Nkx2.5* was expressed at normal levels, and we observed robust expression of the myosin light chain (*MLC2V)* gene (compare Figures 5I and 5J), a target of *Nkx2.5* regulation and early marker of ventricular differentiation (O'Brien et al., 1993; Lyons et al., 1995).

Control of Somite Patterning by Shh and Ihh

Patterning of the vertebrate somite is thought to be regulated by a complex network of signals secreted

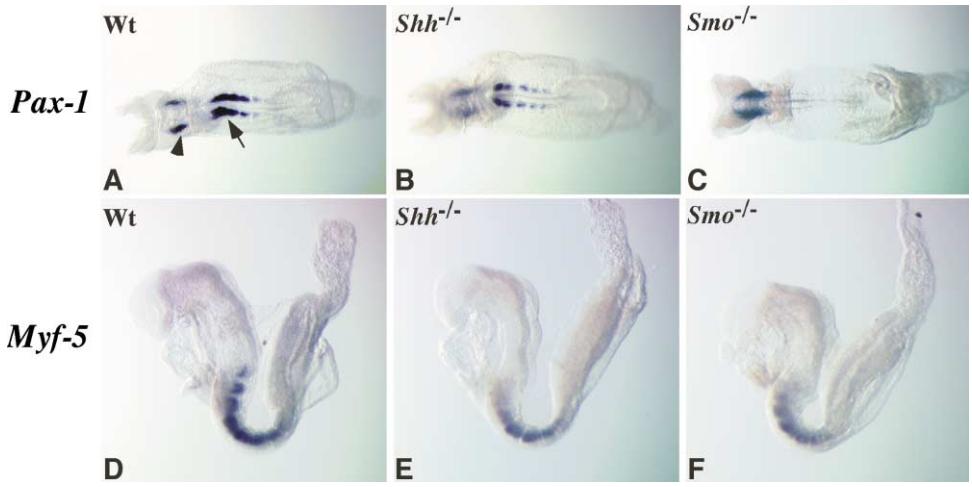

Figure 6. HH Signaling Is Absolutely Required for Expression of the Sclerotomal Determinant *Pax1*, but Not for Activation of the Muscle Determinant *Myf5*

Whole-mount in situ hybridization at the 10 somite stage. (A and D) wild-type embryos; (B and E) *Shh* mutant embryos; (C and F) *Smo* mutant embryos. (A)–(C) are ventral views (anterior to the left) and (D)–(F) are lateral views (anterior to the left). *Pax1* expression in the pharyngeal endoderm is indicated by an arrowhead and expression in the somite by an arrow.

by distinct signaling centers (reviewed in Borycki and Emerson, 2000; Dockter, 2000). For example, sclerotomal development in the ventral medial somite depends upon inductive signals provided by the notochord and floor plate. Both these tissues express *Shh*, and Shh will substitute for these midline tissues in activating the sclerotomal determinant *Pax1* (Fan and Tessier-Lavigne, 1994; Borycki et al., 1998; Teillet et al., 1998; Marcelle et al., 1999; Murtaugh et al., 1999). Thus, Shh has been postulated to play a primary role in the induction of sclerotomal cell fates. However, *Pax1* expression is initiated, albeit at reduced levels, in the somites of *Shh* mutants at the 10 somite stage (Figures 6A and 6B; Chiang et al., 1996); subsequently, *Pax1*-expressing cells undergo apoptosis. These findings suggest that Shh signaling may be essential for maintenance, but not activation, of *Pax1*. Alternatively, there may be redundant mechanisms by which *Pax1* expression is initiated in the somite in vivo.

In support of the latter view, our analysis of *Ptc1* expression indicated that Smo-dependent HH signaling was still occurring within the somite of *Shh* mutants (Figure 2N). In contrast, no activation of *Ptc1* was observed in *Smo* mutants (Figure 2O). *Ihh* expression in the developing embryonic gut or yolk sac endoderm could provide an additional source of HH signal to the somite. Consistent with this model, no activation of *Pax1* was observed in the somite of *Smo* mutant embryos at the 10 somite stage whereas *Pax1* expression in the pharyngeal endoderm was unaltered (Figure 6C). Similar results were obtained with *Bapx1*, a second sclerotomal marker (data not shown). Thus, there is an absolute requirement for HH signaling in sclerotome development, a role normally shared by Shh and Ihh.

Shh signaling has also been implicated in induction of myotomal lineages. Here, epaxial muscles of the back develop from the dorsal medial lip of the somite. One of the first genes to be activated at early somite stages (8.5 dpc) in this epaxial muscle pathway is the myogenic gene, *Myf5*. *Myf5* is also expressed, but only at later stages (9.5 dpc), in hypaxial muscle precursors that arise from the ventro-lateral lip of the somite. *Myf5* expression is upregulated in response to Shh and Wnt signals leading to the proposal that the combined action of these signals initiates *Myf5* activation in epaxial muscle precursors (reviewed in Lassar and Munsterberg, 1996; Cossu and Borello, 1999). *Shh* mutants activate *Myf5* in the 10 somite stage embryo, although at reduced levels (Figures 6D and 6E; Chiang et al., 1996; Borycki et al., 1999). Interestingly, the myotomal phenotype was not enhanced in *Smo* mutants (Figure 6F). Thus, induction of epaxial muscle precursors at early somite stages does not appear to be absolutely dependent on HH signaling.

Discussion

The Mammalian HH Pathway

A number of general conclusions can be drawn from these genetic studies of mammalian HH pathway components. Firstly, Shh and Ihh have redundant signaling functions in the establishment of L/R asymmetry, heart development, somite patterning, and gut closure. Thus, it is likely that these ligands have similar signaling activities. Secondly, a single mammalian *Smo* gene is essential for the transduction of both these signals. Given the absence of a second *Smo* gene in the mammalian genome, we expect Smo will play a similar role in Dhh signaling. The recent analysis of a mutation that maps close to the single *Smo* gene of the zebrafish is consistent with the possibility that multiple HH family members also signal via Smo in the fish (Barresi et al., 2000). Thirdly, *Smo* is epistatic to *Ptc1*, demonstrating an important conservation in the regulatory interactions between HH pathway components from flies to mice.

An Essential Role for HH Signaling in Regulation of L/R Asymmetry

Our current molecular understanding of the mechanisms that govern L/R asymmetry in the vertebrate embryo

stem from the ground-breaking studies of Shh signaling in the developing chick embryo (Levin et al., 1995). In the chick, *Shh* is asymmetrically expressed in the node prior to overt signs of L/R situs. *Nodal*, an apparent target of Shh signaling, is expressed in mesoderm immediately adjacent to the left half of the node, and more broadly in the left lateral plate mesoderm. Blocking Shh signaling, with a monoclonal antibody raised against mouse Shh, prevented left-side specific expression of *Nodal*. In contrast, ectopic Shh on the right side of the embryo lead to ectopic activation of *Nodal* in the right lateral plate mesoderm, and consequently bilateral *Nodal* expression. Importantly, loss of *Nodal* expression on the left side, or bilateral expression, both result in a randomization of heart looping. Thus, a Shh/Nodal signaling pathway is not required for establishing L/R asymmetry, but for ensuring that the process is nonrandom.

Subsequent studies in the chick suggest that Caronte, a likely BMP antagonist activated by Shh, is responsible for relaying the initial Shh signal through the paraxial mesoderm, resulting in the activation of *Nodal* expression in the left lateral plate mesoderm (reviewed in Capdevila et al., 2000). Nodal is thought to regulate a highly conserved pathway of signaling that culminates in left-sided expression of the transcriptional regulator *Pitx2*, a factor essential for the normal situs of several organs (reviewed in Burdine and Schier, 2000; Capdevila et al., 2000). Antagonism of Nodal action by two distantly related TGFβ family members, Lefty1 and 2, is postulated to restrict Nodal signaling to the left side (Lefty1) and modulate Nodal signaling in the left flank (Lefty2) (Meno et al., 1997, 1998). Further, Nodal signaling requires an essential cofactor, Cryptic, an EGF-CFC protein whose function is conserved from fish to mice (reviewed in Shen and Schier, 2000).

In contrast to the chick, *Shh* is not asymmetrically expressed in the mouse node nor is there any evidence of asymmetric HH signaling. For example, *Ptc1*, a general transcriptional target, is broadly expressed in the early somite stage mouse embryo, but its expression is bilaterally symmetric about the midline. Although *Shh* mutants do exhibit bilateral expression of *Nodal* and randomized heart looping (Meyers and Martin; Tsukui et al., 1999), this phenotype appears to be due to a failure of Shh-mediated induction of the floor plate. In the absence of floor plate, there is a secondary loss of floor plate-derived Lefty1, which is required to prevent ectopic activation of *Nodal* in the right lateral plate mesoderm (Meno et al., 1998; Meyers and Martin, 1999; Tsukui et al., 1999). Indeed, several other mutants that disrupt midline patterning display a similar randomization of L/R situs (reviewed in Burdine and Schier, 2000; Capdevila et al., 2000).

Our studies support a direct role for HH signaling in the control of L/R situs in mammals. When both Shh and Ihh signaling are removed, in *Shh/Ihh* compound mutants or *Smo* mutants, *Nodal* is expressed in the node, but not the left lateral plate mesoderm of early somite stage embryos (the time when molecular asymmetry is first observed). As a consequence, there is a complete failure of the left-side program of development. The apparently normal bilateral expression of other genes within the lateral plate mesoderm indicates that the absence of Nodal and downstream targets is a specific phenotype. The failure to initiate *Nodal* expression in the lateral plate mesoderm supports a role for HH signaling in the earliest aspects of L/R control. The demonstration that Shh and Ihh signal within the node is particularly intriguing in this regard.

The node is thought to play dual roles in the control of laterality in the mouse through the production of lateralizing signals and directing their asymmetric distribution by cilial movement within the node (Nonaka et al., 1998). Several lateralizing factors are uniformly expressed in the node. In addition to *Shh* and *Ihh*, the mouse node expresses *Nodal*, its cofactor Cryptic, *Fgf8*, and *Gdf1*. All of these genes also have expression domains outside of the node. Therefore, in the absence of genetic tools that specifically remove node-derived signals, there is some ambiguity as to the actual source of the signals controlling L/R situs. Interestingly, *Gdf1* and *Fgf8* mutants both fail to activate *Nodal* in the left lateral plate mesoderm, suggesting that either, or both, of these factors may be targets of HH signaling (Meyers and Martin, 1999; Rankin et al., 2000). Our data indicate that expression of *Gdf1,* but not *Fgf8* (data not shown), in the mouse node is HH dependent. *Gdf1* is downregulated in *Smo* mutants and upregulated in *Ptc1* mutants. Thus, HH signaling in the node appears to lie upstream of *Gdf1*, suggesting that at least part of the laterality defects we observe can be explained by loss of *Gdf1* activity. However, the failure of *Nodal* induction in the left lateral plate mesoderm is fully penetrant in *Smo*, but not *Gdf1*, mutants (Rankin et al., 2000). Thus, there are likely to be mechanisms other than the control of *Gdf1* expression by which HH signaling regulates activity of the node. In support of this view, we observe reduced expression of *Nodal* and *Cryptic* in *Smo* mutants. At the gross structural level, the node appears morphologically normal and expresses several genes that are not implicated directly in the regulation of situs (for example *Brachyury*; data not shown). Further, the notochord, which is derived from the node, forms in *Smo* mutants (Figure 1H), indicating that this aspect of node function is intact. Preliminary scanning electron microscopy indicates that node cilia are present and appear similar to those of wild-type embryos (data not shown). However, we have not attempted to measure cilial-based nodal flow in *Smo* mutants.

Taken together with other studies, our findings support the model outlined in Figure 7. Either Shh or Ihh signaling is required for activation of *Gdf1* and for establishing normal levels of expression of *Nodal* in the node. As a result of defective node signaling, no left-side pathway of development is initiated. Whether there is also a right-sided pathway and, if so, what happens to expression of these genes in the absence of HH signaling remains an open question. Unfortunately, no genes have been reported that are only expressed on the right side of the mouse embryo at equivalent stages.

The finding that Shh and Ihh play redundant roles suggests that the chick and mouse may utilize similar pathways to initiate L/R development. Indeed, the antibody used in Shh blocking experiments in the chick embryo (Levin et al., 1995) actually recognizes both Shh and Ihh in the mouse, raising the possibility that the chick manipulations may have inhibited both Shh and

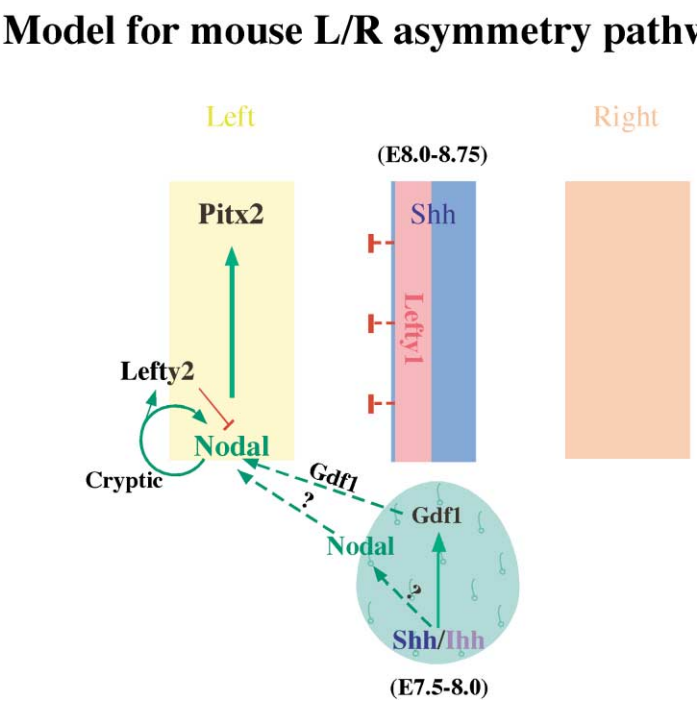

Figure 7. Model for the Role of HH Signaling in Regulation of L/R Asymmetry in the Mouse

Shh and Ihh signaling in the mouse node acts upstream of *Gdf1*, which is required for the induction of asymmetric gene expression in the left lateral plate mesoderm. HH signaling is also required, most likely indirectly, for normal levels of *Nodal* expression in the node. Whether node-derived *Nodal* plays a role in the regulation of L/R asymmetry is not currently known.

Ihh signaling. However, studies in the chick indicate that activation of HH signaling in the right lateral plate mesoderm is sufficient to ectopically activate *Nodal* and a left-side specific pathway whereas in the mouse, it is not, as constitutive activation of HH signaling in *Ptc1* mutants does not alter *Nodal* expression. Thus, it appears that in the chick, HH signaling may play a direct role outside of the node in regulating the left pathway of factors in adjacent mesodermal populations whereas in the mouse, HH signaling within the node may be the key regulatory event.

Hedgehog Signaling and Heart Development

Although the loss of left-side marker expression in *Smo* mutants can largely be explained by the loss of *Gdf1*, *Gdf1* mutant embryos undergo heart looping, albeit in a randomized direction. In contrast, the heart of a *Smo* mutant remains as a linear midline tube. Indeed, almost all mutants in L/R situs still undergo looping morphogenesis of the heart (Burdine and Schier, 2000). Thus, L/R signaling does not appear to directly regulate looping per se, but rather to bias this process so that normally only rightward looping occurs. We suggest that the severe linear heart tube defect observed in *Smo* mutants may reflect a distinct role for HH signaling in cardiac morphogenesis. In support of this argument, heart tube formation was significantly delayed in *Smo* mutants, which is not the case in other mutants where the regulation of L/R asymmetry is disrupted. Correlated with this delay, expression of *Nkx2.5*, a transcriptional regulator essential for heart looping (Lyons et al., 1995), was barely detectable in the cardiac region of head-fold stage *Smo* mutant embryos. These observations suggest a possible link between HH signaling and *Nkx2.5* regulation. However, *Ptc1* expression is not observed in heart precursors at this time (data not shown), suggesting that the cardiac tube is not directly responding to HH signaling or that HH signaling may act at an earlier stage of cardiac development. Cardiac precursors originate from the anterior primitive streak (Lyons, 1996) where they may be exposed to HH signaling from the node (both Shh and Ihh) and visceral endoderm (Ihh only). Alternatively, cardiac precursors may receive Shh and Ihh signals from the definitive endoderm, a tissue known to regulate cardiac development. By 9.0 dpc, *Smo* mutants express normal levels of *Nkx2.5*, suggesting that there may be both HH-dependent and HH-independent phases in *Nkx2.5* regulation. At this stage, we also observe appropriate regulation of *MCL2V*, a ventricular target of *Nkx2.5* (Lyons et al., 1995). Thus, *Smo* mutant hearts appear to undergo ventricular differentiation despite the initial delay in cardiac development and failure of looping morphogenesis.

A Role for Ihh in Somite Patterning

Earlier work has shown that midline signals, from the notochord and ventral neural tube, are required for induction of sclerotome, the precursors of the axial skeleton (reviewed in Dockter, 2000). The demonstration that Shh induces sclerotomal markers and can substitute for axial tissues in this role suggests that Shh is the midline signal. However, although *Shh* mutants have no axial skeleton, examination of the sclerotomal marker *Pax1* indicated that sclerotomal cells were initially specified, but underwent cell death at later stages (Chiang et al., 1996). This has led to the proposal that Shh is a mitogen/survival factor for the sclerotome and not its inducer (Teillet et al., 1998). Our data indicate that *Ptc1* remains upregulated in the somites of *Shh* mutants, indicating that Shh-independent signaling is likely to be occurring. *Ihh* is expressed in endoderm and visceral endoderm that underlie the somites. Therefore, it is well positioned

to also play a role in somite patterning. Indeed, the removal of all HH signaling in *Smo* mutants leads to a complete absence of *Pax1* expressing sclerotome, in support of an additional role for Ihh in specification of the sclerotomal lineage.

Shh is also implicated in the induction of the dorsomedial myotomal cells that give rise to the epaxial back musculature. This population, which can first be recognized by expression of *Myf5* at 8.5 dpc, is present but reduced in *Shh* mutants at this stage. In contrast to the sclerotome, the myotomal phenotype is not enhanced in *Smo* mutants, if embryos are examined shortly after the initiation of *Myf5* expression. Thus, it appears that somite patterning is likely to involve different HHs acting in different regions of the somite at different stages of somite development. In the newly formed somite, Shh produced by notochord, along with Ihh and Shh produced by endoderm cell types, are responsible for induction of the sclerotome. Long-term survival of the sclerotome depends on Shh signaling, most likely from the notochord and floor plate. Induction of the dorsal myotome utilizes Shh, in conjunction with members of the Wnt family (reviewed in Borycki and Emerson, 2000). However, whereas there is an absolute requirement for HH signaling to induce sclerotome, there does not appear to be an absolute requirement for HH signaling in the induction of myotome at early somite stages.

Experimental Procedures

Mice

Generation of *Shh*, *Ihh*, and *Ptc1* mutant embryos has been described (Goodrich et al., 1997; St-Jacques et al., 1998, 1999). *Ptc1*^{lacZ} mice were kindly provided by Matthew Scott (Goodrich et al., 1997). Mutations were studied on mixed (129/Sv; Swiss Black and 129/Sv; C57BL6/J;CBA/J) and inbred (129/Sv) backgrounds. No difference in the *Smo* mutant phenotype was observed on these backgrounds. Noon of the day of detection of the vaginal plug was considered as 0.5 days post coitum.

Generation of *Smo* Mutants

A complete description of the targeting vector construct, chimera production, and allele identification is provided elsewhere (see Supplementary Experimental Procedures online at http://www.cell.com/cgi/content/full/105/6/781/DC1). Briefly, a null allele at the *Smo* locus was generated in the AV3 ES cell line (G. Vassileva and A.P.M., unpublished data) by replacing sequences 44 bp upstream and 358 bp downstream of the initiation ATG of the *Smo* gene by a *PGKneo*-positive selection cassette. Correctly targeted ES cells were identified by Southern blot hybridization and chimeras generated by blastocyst injection. Chimeric males were bred with 129/Sv or Black Swiss females. Heterozygous offspring were identified by either Southern blotting or PCR of tail-tip DNA. Embryos homozygous for the *Smo* null mutation were obtained from heterozygous intercrosses. Genomic DNA prepared from yolk sac was genotyped by PCR. Primers specific for the wild-type and mutant alleles were used in separate PCR reactions.

In Situ Hybridization and Histology

For a description of in situ hybridization probes and procedures see Supplementary Experimental Procedures on the *Cell* website. Wild-type and mutant embryos were dissected in PBS, fixed overnight in 4% paraformaldehyde in PBS or Bouin's fixative, wax embedded, and 6 μm sections prepared. Hematoxylin and eosin staining was performed using standard histology techniques. Whole-mount β-galactosidase detection was performed as described (Whiting et al., 1991).

Acknowledgments

We thank M. Scott, J.C. Izpisúa Belmonte, E. Robertson, H. Hamada, Se-Jin Lee, M. Shen, R. Harvey, T. Lufkin, R. Harland, R. Krumlauf, B. Hogan, R. Behringer, and H. Akiyama for supplying cDNA probes; Jill McMahon for ES cell injection; Diane Faria for histology. We also thank Paula Lewis, Mark Wijgerde, and Terry Yamaguchi for critical input. X.M.Z. gratefully acknowledges support from Ontogeny Inc. (now Curis Inc.). M.R.-S. was supported in part by the Praxis XXI Program, Foundation for Science and Technology, Portugal and wishes to thank Maria Irene Ramalho, Boaventura Sousa Santos, João Ramalho-Santos, and Cássia Calebaut Mendes for their encouragement. This work was supported by a grant from the National Institute of Neurological Disorders and Stroke at the NIH (NS33642).

Received March 20, 2001; revised May 17, 2001.

References

Akiyama, H., Shigeno, C., Hiraki, Y., Shukunami, C., Kohno, H., Akagi, M., Konishi, J., and Nakamura, T. (1997). Cloning of a mouse smoothened cDNA and expression patterns of hedgehog signalling molecules during chondrogenesis and cartilage differentiation in clonal mouse EC cells, ATDC5. Biochem. Biophys. Res. Commun. *235*, 142–147.

Alcedo, J., Zou, Y., and Noll, M. (2000). Post-transcriptional regulation of smoothened is part of a self- correcting mechanism in the Hedgehog signaling system. Mol. Cell *6*, 457–465.

Apelqvist, A., Ahlgren, U., and Edlund, H. (1997). Sonic hedgehog directs specialised mesoderm differentiation in the intestine and pancreas. Curr. Biol. *7*, 801–804.

Barresi, M.J., Stickney, H.L., and Devoto, S.H. (2000). The zebrafish slow-muscle-omitted gene product is required for Hedgehog signal transduction and the development of slow muscle identity. Development *127*, 2189–2199.

Bitgood, M.J., and McMahon, A.P. (1995). Hedgehog and Bmp genes are coexpressed at many diverse sites of cell-cell interaction in the mouse embryo. Dev. Biol. *172*, 126–138.

Bitgood, M.J., Shen, L., and McMahon, A.P. (1996). Sertoli cell signaling by Desert hedgehog regulates the male germline. Curr. Biol. *6*, 298–304.

Borycki, A.G., and Emerson, C.P., Jr. (2000). Multiple tissue interactions and signal transduction pathways control somite myogenesis. Curr. Top. Dev. Biol. *48*, 165–224.

Borycki, A.G., Brunk, B., Tajbakhsh, S., Buckingham, M., Chiang, C., and Emerson, C.P., Jr. (1999). Sonic hedgehog controls epaxial muscle determination through Myf5 activation. Development *126*, 4053–4063.

Borycki, A.G., Mendham, L., and Emerson, C.P., Jr. (1998). Control of somite patterning by Sonic hedgehog and its downstream signal response genes. Development *125*, 777–790.

Burdine, R.D., and Schier, A.F. (2000). Conserved and divergent mechanisms in left-right axis formation. Genes Dev. *14*, 763–776.

Capdevila, J., Vogan, K.J., Tabin, C.J., and Izpisua Belmonte, J.C. (2000). Mechanisms of left-right determination in vertebrates. Cell *101*, 9–21.

Carpenter, D., Stone, D.M., Brush, J., Ryan, A., Armanini, M., Frantz, G., Rosenthal, A., and de Sauvage, F.J. (1998). Characterization of two patched receptors for the vertebrate hedgehog protein family. Proc. Natl. Acad. Sci. USA *95*, 13630–13634.

Chen, Y., and Struhl, G. (1996). Dual roles for patched in sequestering and transducing hedgehog. Cell *87*, 553–563.

Chiang, C., Litingtung, Y., Lee, E., Young, K.E., Corden, J.L., Westphal, H., and Beachy, P.A. (1996). Cyclopia and defective axial patterning in mice lacking Sonic hedgehog gene function. Nature *383*, 407–413.

Chiang, C., Swan, R.Z., Grachtchouk, M., Bolinger, M., Litingtung, Y., Robertson, E.K., Cooper, M.K., Gaffield, W., Westphal, H., Beachy, P.A., and Dlugosz, A.A. (1999). Essential role for Sonic hedgehog during hair follicle morphogenesis. Dev. Biol. *205*, 1–9.

Collignon, J., Varlet, I., and Robertson, E.J. (1996). Relationship between asymmetric nodal expression and the direction of embryonic turning. Nature *381*, 155–158.

Cossu, G., and Borello, U. (1999). Wnt signaling and the activation of myogenesis in mammals. EMBO J. *18*, 6867–6872.

Dassule, H.R., and McMahon, A.P. (1998). Analysis of epithelial-mesenchymal interactions in the initial morphogenesis of the mammalian tooth. Dev. Biol. *202*, 215–227.

Dassule, H.R., Lewis, P., Bei, M., Maas, R., and McMahon, A.P. (2000). Sonic hedgehog regulates growth and morphogenesis of the tooth. Development *127*, 4775–4785.

Denef, N., Neubuser, D., Perez, L., and Cohen, S.M. (2000). Hedgehog induces opposite changes in turnover and subcellular localization of patched and smoothened. Cell *102*, 521–531.

Dockter, J.L. (2000). Sclerotome induction and differentiation. Curr. Top. Dev. Biol. *48*, 77–127.

Dutton, R., Yamada, T., Turnley, A., Bartlett, P.F., and Murphy, M. (1999). Sonic hedgehog promotes neuronal differentiation of murine spinal cord precursors and collaborates with neurotrophin 3 to induce Islet-1. J. Neurosci. *19*, 2601–2608.

Echelard, Y., Epstein, D.J., St-Jacques, B., Shen, L., Mohler, J., McMahon, J.A., and McMahon, A.P. (1993). Sonic hedgehog, a member of a family of putative signaling molecules, is implicated in the regulation of CNS polarity. Cell *75*, 1417–1430.

Fan, C.M., and Tessier-Lavigne, M. (1994). Patterning of mammalian somites by surface ectoderm and notochord: evidence for sclerotome induction by a hedgehog homolog. Cell *79*, 1175–1186.

Fan, C.M., Porter, J.A., Chiang, C., Chang, D.T., Beachy, P.A., and Tessier-Lavigne, M. (1995). Long-range sclerotome induction by sonic hedgehog: direct role of the amino-terminal cleavage product and modulation by the cyclic AMP signaling pathway. Cell *81*, 457–465.

Gaio, U., Schweickert, A., Fischer, A., Garratt, A.N., Muller, T., Ozcelik, C., Lankes, W., Strehle, M., Britsch, S., Blum, M., and Birchmeier, C. (1999). A role of the cryptic gene in the correct establishment of the left- right axis. Curr. Biol. *9*, 1339–1342.

Goodrich, L.V., Milenkovic, L., Higgins, K.M., and Scott, M.P. (1997). Altered neural cell fates and medulloblastoma in mouse patched mutants. Science *277*, 1109–1113.

Hammerschmidt, M., Brook, A., and McMahon, A.P. (1997). The world according to hedgehog. Trends Genet. *13*, 14–21.

Hebrok, M., Kim, S.K., St Jacques, B., McMahon, A.P., and Melton, D.A. (2000). Regulation of pancreas development by hedgehog signaling. Development *127*, 4905–4913.

Hynes, M., Ye, W., Wang, K., Stone, D., Murone, M., Sauvage, F., and Rosenthal, A. (2000). The seven-transmembrane receptor smoothened cell-autonomously induces multiple ventral cell types. Nat. Neurosci. *3*, 41–46.

Ingham, P.W., Nystedt, S., Nakano, Y., Brown, W., Stark, D., van den Heuvel, M., and Taylor, A.M. (2000). Patched represses the hedgehog signaling pathway by promoting modification of the Smoothened protein. Curr. Biol. *10*, 1315–1318.

Karp, S.J., Schipani, E., St-Jacques, B., Hunzelman, J., Kronenberg, H., and McMahon, A.P. (2000). Indian hedgehog coordinates endochondral bone growth and morphogenesis via parathyroid hormone related-protein-dependent and -independent pathways. Development *127*, 543–548.

Kos, L., Chiang, C., and Mahon, K.A. (1998). Mediolateral patterning of somites: multiple axial signals, including Sonic hedgehog, regulate Nkx-3.1 expression. Mech. Dev. *70*, 25–34.

Lassar, A.B., and Munsterberg, A.E. (1996). The role of positive and negative signals in somite patterning. Curr. Opin. Neurobiol. *6*, 57–63.

Levin, M., Johnson, R.L., Stern, C.D., Kuehn, M., and Tabin, C. (1995). A molecular pathway determining left-right asymmetry in chick embryogenesis. Cell *82*, 803–814.

Litingtung, Y., Lei, L., Westphal, H., and Chiang, C. (1998). Sonic hedgehog is essential to foregut development. Nat. Genet. *20*, 58–61.

Liu, A., Joyner, A.L., and Turnbull, D.H. (1998). Alteration of limb and brain patterning in early mouse embryos by ultrasound-guided injection of Shh-expressing cells. Mech. Dev. *75*, 107–115.

Lyons, G.E. (1996). Vertebrate heart development. Curr. Opin. Genet. Dev. *6*, 454–460.

Lyons, I., Parsons, L.M., Hartley, L., Li, R., Andrews, J.E., Robb, L., and Harvey, R.P. (1995). Myogenic and morphogenetic defects in the heart tubes of murine embryos lacking the homeo box gene Nkx2–5. Genes Dev. *9*, 1654–1666.

Marcelle, C., Ahlgren, S., and Bronner-Fraser, M. (1999). In vivo regulation of somite differentiation and proliferation by Sonic Hedgehog. Dev. Biol. *214*, 277–287.

Marigo, V., Davey, R.A., Zuo, Y., Cunningham, J.M., and Tabin, C.J. (1996). Biochemical evidence that patched is the Hedgehog receptor. Nature *384*, 176–179.

Masuya, H., Sagai, T., Wakana, S., Moriwaki, K., and Shiroishi, T. (1995). A duplicated zone of polarizing activity in polydactylous mouse mutants. Genes Dev. *9*, 1645–1653.

Meno, C., Ito, Y., Saijoh, Y., Matsuda, Y., Tashiro, K., Kuhara, S., and Hamada, H. (1997). Two closely-related left-right asymmetrically expressed genes, lefty-1 and lefty-2: their distinct expression domains, chromosomal linkage and direct neuralizing activity in Xenopus embryos. Genes Cells *2*, 513–524.

Meno, C., Shimono, A., Saijoh, Y., Yashiro, K., Mochida, K., Ohishi, S., Noji, S., Kondoh, H., and Hamada, H. (1998). lefty-1 is required for left-right determination as a regulator of lefty-2 and nodal. Cell *94*, 287–297.

Meyers, E.N., and Martin, G.R. (1999). Differences in left-right axis pathways in mouse and chick: functions of FGF8 and SHH. Science *285*, 403–406.

Monkley, S.J., Delaney, S.J., Pennisi, D.J., Christiansen, J.H., and Wainwright, B.J. (1996). Targeted disruption of the Wnt2 gene results in placentation defects. Development *122*, 3343–3353.

Murtaugh, L.C., Chyung, J.H., and Lassar, A.B. (1999). Sonic hedgehog promotes somitic chondrogenesis by altering the cellular response to BMP signaling. Genes Dev. *13*, 225–237.

Nonaka, S., Tanaka, Y., Okada, Y., Takeda, S., Harada, A., Kanai, Y., Kido, M., and Hirokawa, N. (1998). Randomization of left-right asymmetry due to loss of nodal cilia generating leftward flow of extraembryonic fluid in mice lacking KIF3B motor protein. Cell *95*, 829–837.

O'Brien, T.X., Lee, K.J., and Chien, K.R. (1993). Positional specification of ventricular myosin light chain 2 expression in the primitive murine heart tube. Proc. Natl. Acad. Sci. USA *90*, 5157–5161.

Parmantier, E., Lynn, B., Lawson, D., Turmaine, M., Namini, S.S., Chakrabarti, L., McMahon, A.P., Jessen, K.R., and Mirsky, R. (1999). Schwann cell-derived Desert hedgehog controls the development of peripheral nerve sheaths. Neuron *23*, 713–724.

Parr, B.A., and McMahon, A.P. (1995). Dorsalizing signal Wnt-7a required for normal polarity of D-V and A-P axes of mouse limb. Nature *374*, 350–353.

Pepicelli, C.V., Lewis, P.M., and McMahon, A.P. (1998). Sonic hedgehog regulates branching morphogenesis in the mammalian lung. Curr. Biol. *8*, 1083–1086.

Piedra, M.E., Icardo, J.M., Albajar, M., Rodriguez-Rey, J.C., and Ros, M.A. (1998). Pitx2 participates in the late phase of the pathway controlling left-right asymmetry. Cell *94*, 319–324.

Quirk, J., van den Heuvel, M., Henrique, D., Marigo, V., Jones, T.A., Tabin, C., and Ingham, P.W. (1997). The smoothened gene and hedgehog signal transduction in Drosophila and vertebrate development. Cold Spring Harb. Symp. Qunat. Biol. *62*, 217–226.

Ramalho-Santos, M., Melton, D.A., and McMahon, A.P. (2000). Hedgehog signals regulate multiple aspects of gastrointestinal development. Development *127*, 2763–2772.

Ramirez-Weber, F.A., Casso, D.J., Aza-Blanc, P., Tabata, T., and Kornberg, T.B. (2000). Hedgehog signal transduction in the posterior compartment of the Drosophila wing imaginal disc. Mol. Cell *6*, 479–485.

Rankin, C.T., Bunton, T., Lawler, A.M., and Lee, S.J. (2000). Regula-

tion of left-right patterning in mice by growth/differentiation factor-1. Nat. Genet. *24*, 262–265.

Rowitch, D.H., St-Jacques, B., Lee, S.M., Flax, J.D., Snyder, E.Y., and McMahon, A.P. (1999). Sonic hedgehog regulates proliferation and inhibits differentiation of CNS precursor cells. J. Neurosci. *19*, 8954–8965.

Ryan, A.K., Blumberg, B., Rodriguez-Esteban, C., Yonei-Tamura, S., Tamura, K., Tsukui, T., de la Pena, J., Sabbagh, W., Greenwald, J., Choe, S., et al. (1998). Pitx2 determines left-right asymmetry of internal organs in vertebrates. Nature *394*, 545–551.

Sarkar, L., Cobourne, M., Naylor, S., Smalley, M., Dale, T., and Sharpe, P.T. (2000). Wnt/Shh interactions regulate ectodermal boundary formation during mammalian tooth development. Proc. Natl. Acad. Sci. USA *97*, 4520–4524.

Sato, N., Leopold, P.L., and Crystal, R.G. (1999). Induction of the hair growth phase in postnatal mice by localized transient expression of Sonic hedgehog. J. Clin. Invest. *104*, 855–864.

Shen, M.M., and Schier, A.F. (2000). The EGF-CFC gene family in vertebrate development. Trends Genet. *16*, 303–309.

St-Jacques, B., Dassule, H.R., Karavanova, I., Botchkarev, V.A., Li, J., Danielian, P.S., McMahon, J.A., Lewis, P.M., Paus, R., and McMahon, A.P. (1998). Sonic hedgehog signaling is essential for hair development. Curr. Biol. *8*, 1058–1068.

St-Jacques, B., Hammerschmidt, M., and McMahon, A.P. (1999). Indian hedgehog signaling regulates proliferation and differentiation of chondrocytes and is essential for bone formation. Genes Dev. *13*, 2072–2086.

Stone, D.M., Hynes, M., Armanini, M., Swanson, T.A., Gu, Q., Johnson, R.L., Scott, M.P., Pennica, D., Goddard, A., Phillips, H., et al. (1996). The tumour-suppressor gene patched encodes a candidate receptor for Sonic hedgehog. Nature *384*, 129–134.

Strutt, H., Thomas, C., Stark, D., Neave, B., Taylor, A.M., and Ingham, P.W. (2001). Mutations in the sterol sensing domain of patched suggest a role for vesicular trafficking in smoothened regulation. Curr. Biol. *11*, 608–613.

Teillet, M., Watanabe, Y., Jeffs, P., Duprez, D., Lapointe, F., and Le Douarin, N.M. (1998). Sonic hedgehog is required for survival of both myogenic and chondrogenic somitic lineages. Development *125*, 2019–2030.

Tsukui, T., Capdevila, J., Tamura, K., Ruiz-Lozano, P., Rodriguez-Esteban, C., Yonei-Tamura, S., Magallon, J., Chandraratna, R.A., Chien, K., Blumberg, B., et al. (1999). Multiple left-right asymmetry defects in Shh(−/−) mutant mice unveil a convergence of the shh and retinoic acid pathways in the control of Lefty-1. Proc. Natl. Acad. Sci. USA *96*, 11376–11381.

Vortkamp, A., Lee, K., Lanske, B., Segre, G.V., Kronenberg, H.M., and Tabin, C.J. (1996). Regulation of rate of cartilage differentiation by Indian hedgehog and PTH-related protein. Science *273*, 613–622.

Wallace, V.A. (1999). Purkinje-cell-derived Sonic hedgehog regulates granule neuron precursor cell proliferation in the developing mouse cerebellum. Curr. Biol. *9*, 445–448.

Wechsler-Reya, R.J., and Scott, M.P. (1999). Control of neuronal precursor proliferation in the cerebellum by Sonic Hedgehog. Neuron *22*, 103–114.

Whiting, J., Marshall, H., Cook, M., Krumlauf, R., Rigby, P.W., Stott, D., and Allemann, R. (1991). Multiple spatially specific enhancers are required to reconstruct the pattern of Hox-2.6 gene expression. Genes Dev. *5*, 2048–2059.

Xie, J., Murone, M., Luoh, S.M., Ryan, A., Gu, Q., Zhang, C., Bonifas, J.M., Lam, C.W., Hynes, M., Goddard, A., et al. (1998). Activating Smoothened mutations in sporadic basal-cell carcinoma. Nature *391*, 90–92.

Yan, Y.T., Gritsman, K., Ding, J., Burdine, R.D., Corrales, J.D., Price, S.M., Talbot, W.S., Schier, A.F., and Shen, M.M. (1999). Conserved requirement for EGF-CFC genes in vertebrate left-right axis formation. Genes Dev. *13*, 2527–2537.

Ye, W., Shimamura, K., Rubenstein, J.L., Hynes, M.A., and Rosenthal, A. (1998). FGF and Shh signals control dopaminergic and serotonergic cell fate in the anterior neural plate. Cell *93*, 755–766.

Yoshioka, H., Meno, C., Koshiba, K., Sugihara, M., Itoh, H., Ishimaru, Y., Inoue, T., Ohuchi, H., Semina, E.V., Murray, J.C., et al. (1998). Pitx2, a bicoid-type homeobox gene, is involved in a lefty-signaling pathway in determination of left-right asymmetry. Cell *94*, 299–305.

Zhang, Y., Zhang, Z., Zhao, X., Yu, X., Hu, Y., Geronimo, B., Fromm, S.H., and Chen, Y.P. (2000). A new function of BMP4: dual role for BMP4 in regulation of Sonic hedgehog expression in the mouse tooth germ. Development *127*, 1431–1443.

Zuniga, A., Haramis, A.P., McMahon, A.P., and Zeller, R. (1999). Signal relay by BMP antagonism controls the SHH/FGF4 feedback loop in vertebrate limb buds. Nature *401*, 598–602.